CRITICAL VELOCITY IN OPEN CAPILLARY CHANNEL FLOWS

Uwe Rosendahl, Michael E. Dreyer, Hans J. Rath
Center of Applied Space Technology and Microgravity (ZARM)
University of Bremen, Germany

Brian Motil
NASA Glenn Research Center, Cleveland, Ohio

ABSTRACT

We investigate forced liquid flows through open capillary channels with free surfaces experimentally. The experiments were performed under low gravity conditions in the Bremen Drop Tower and on board the sounding rocket TEXUS-37. Open capillary channels (vanes) are used in surface tension tanks to transport the propellant and to provide a flow path for the bubble-free liquid supply to the thrusters. Since the free surfaces can only withstand a certain pressure differential between the liquid and ambient, the flow rate in the channel is limited. The maximum flow rate is achieved when the surfaces collapse and gas is ingested into the outlet. Since experimental and theoretical data of this flow rate limitation is lacking, the safety factors for the application of vanes in surface tension tanks must be unnecessary high.

The aim of the investigation is to determine the maximum liquid flow rate and the corresponding critical flow velocity. The characteristic nondimensional parameters, OHNESORGE number, and gap ratio, cover a wide range of usual vanes. For the theoretical approach a one-dimensional momentum balance was set up. The numerical solution yields the maximum volume flux and the position of the free surface in good agreement with the experiments.

INTRODUCTION

Open capillary channels are used in space to transport and position liquids. An open capillary channel is a structure of arbitrary geometry which establishes a free surface flow when the hydrostatic pressure vanishes and surface tension forces become dominant, e. g. within the compensated gravity environment of an orbiting spacecraft. The free surface of the liquid flow is always exposed to the ambient pressure and the liquid is fixed inside the channel due to capillary forces. Prominent applications are heat pipes and surface tension tanks of satellites. In the latter case, open capillary channels, so called vanes, provide a flow path from the bulk of propellant to the tank outlet or a refillable reservoir. Simple vanes consist of a thin sheet metal mounted parallel or perpendicularly to the tank shell. Whenever the vane is in contact with the propellant the vane fills itself due to the capillary forces. Driven by a gradient of the capillary pressure between the liquid head in the vane and the bulk liquid, the propellant is conducted to the tank outlet. Thus, vanes are a simple device for the direct supply to the tank outlet wherever the bulk propellant is located in the tank.

The major problem of the direct use of vanes is the limitation of the flow rate, which causes the liquid surface to collapse. Since the physics behind the effect of flow rate limitation in open capillary channels is not well-known, the design of vanes is based on estimations. The only work in this field are model computations by Jaekle[1] and Der[2]. To address the lack of experimental data we developed an experiment to investigate the limits of flow rates in open capillary channels.

To identify the problem we consider an open channel as shown in Fig. 1. The channel consists of two parallel plates of distance a, width b and length l. The inlet and the outlet of the channel are each connected to a duct with a closed cross section. A constant volumetric flow Q in the direction of the longitudinal channel axis x is assumed. The liquid flow path is bounded by free surfaces between the edges of the plates. Both liquid surfaces are exposed to the ambient gas pressure p_a, which is kept con-

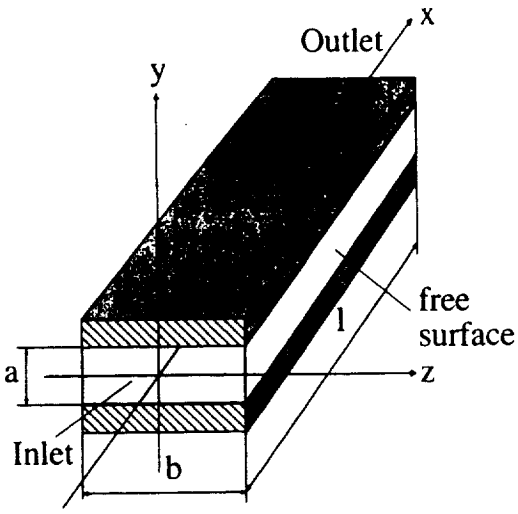

Figure 1: Schematic drawing of the capillary channel consisting of two parallel plates. The volume flux Q through the channel along the flow path x leads to an increasing surface curvature.

stant as well as the temperature. Depending on the applied volume flux, the liquid pressure decreases in the flow direction x due to flow losses. To achieve stationary flow conditions the difference between the liquid pressure p and the ambient pressure p_a has to be balanced by the capillary pressure of the free surface. For that reason the surface curvature increases in the flow direction and the flow path becomes smaller. Since the free surface can only withstand a certain differential pressure, the flow rate in the channel is limited to a certain value. The maximum rate is achieved when the surfaces collapse at the end of the capillary channel and gas ingestion occurs at the channel outlet. The aim of the investigations is to determine the maximum flow rate and the corresponding critical velocities.

THEORETICAL APPROACH

For the analysis we assume a one-dimensional flow along the channel axis x characterized by the mean velocity v and the liquid pressure p (see Fig. 1). The origin of the coordinate system is located in the center of the cross section at the channel inlet. The basic equations to be solved are the momentum equation

$$dp + \rho v dv + dw_f = 0 \tag{1}$$

and the equation of continuity

$$d(Av) = 0, \tag{2}$$

both given in differential form. The term dw_f of Eq. (1) considers the pressure losses due to friction and the change of velocity profile in the entrance region. ρ denotes the density of the liquid and A is the cross section of the flow path perpendicular to the longitudinal axis x. We neglect the hydrostatic pressure since the experiments were operated in an environment of low gravity of $10^{-4}g$ -$10^{-5}g$, with g representing the gravity acceleration on earth.

At first a relation between the liquid pressure and the position of the free surface z is derived. The liquid pressure p is related to the mean curvature H of the free surface by the GAUSS-LAPLACE equation

$$p - p_a = -2\sigma H = -\sigma\left(\frac{1}{R_1} + \frac{1}{R_2}\right). \tag{3}$$

Herein σ is the surface tension, R_1 and R_2 are the principal radii of curvature. Since the ambient pressure p_a is constant the pressure gradient becomes

$$dp = -2\sigma dH. \tag{4}$$

In general, the mean curvature of the surface is calculated by

$$2H(x,y) = \frac{\left(z_x^2+1\right) z_{yy} - 2z_x z_y z_{xy} + \left(1+z_y^2\right) z_{xx}}{\left(1+z_x^2+z_y^2\right)^{\frac{3}{2}}} \tag{5}$$

(see e. g. Bronstein[3]). z is the position of the surface defined by a function $z = f(x,y)$, with $x \in [0,l]$ and $y \in [-a/2, a/2]$. The indices in Eq. (5) denote partial derivatives: $z_i = \partial z/\partial i$, $z_{ij} = \partial^2 z/\partial i \partial j$, with $i,j \in \{x,y\}$. Eq. (5) can be simplified by applying the basic assumption of a one-dimensional flow that the liquid pressure variation is negligible over each cross section. With this assumption the surface curvature in the cross section is constant and defined by the radius of curvature R shown in Fig. 2. In that case the radius R and the cross section area A are calculated from the distance $k(x)$ by geometrical relations

$$R = g_1(k) \tag{6}$$

$$A = g_2(R). \tag{7}$$

k is the innermost line of the surface

$$k(x) = z(x,y)|_{y=0} \tag{8}$$

in the plane of symmetry at $y = 0$, which was detected in the experiment. The simplification of Eq. (5) occurs since the derivative of z with respect to y vanishes along the innermost line

$$\left.\frac{\partial z}{\partial y}\right|_{y=0} = 0. \tag{9}$$

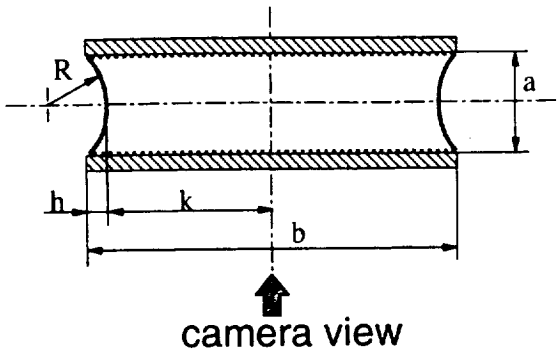

Figure 2: Cross section of the capillary channel with radius of curvature R, contour length k, and surface deformation h. The observation is performed perpendicular to the plates.

With Eq. (8) and Eq. (9) Eq. (5) reduces to

$$2H(x, y=0) = \frac{k_{xx}}{(1+k_x^2)^{\frac{3}{2}}} + \frac{1}{R}\frac{1}{(1+k_x^2)^{\frac{1}{2}}}. \quad (10)$$

With the definition of the volume flux Q from Eq. (2)

$$Q = Av \quad (11)$$

the second term of Eq. (1) can be rewritten as

$$\rho v\, dv = -\rho \frac{Q^2}{A^3} dA. \quad (12)$$

The pressure loss dw_f in Eq. (1) consists of two parts, the laminar viscous pressure loss and the additional entrance pressure loss, which is a result of the change of the velocity profile from the entrance profile to the parabolic velocity distribution (POISEUILLE flow). The pressure loss we apply is

$$dw_f = \frac{\rho Q^2}{2D_h \,\mathrm{Re}_{D_h} A^2} [k_{pf} + k_{pe}]\, dx. \quad (13)$$

Neglecting the factor k_{pe}, Eq. (13) yields the laminar pressure loss for two parallel plates obtained from an exact solution of the NAVIER-STOKES equation (White[4]). Therein $k_{pf} = 96$ is the friction factor, $D_h = 2a$ the hydraulic diameter, and $\mathrm{Re}_{D_h} = D_h v/\nu$ is the REYNOLDS number. The kinematic viscosity is denoted with ν. The additional pressure loss due to the transformation of the entrance velocity profile to the laminar parabolic velocity distribution is taken into account by the factor k_{pe}. This factor, which is not discussed in detail in this paper, was derived from an analytical relation of the entrance pressure loss in a channel of two parallel plates proposed by Sparrow et. al.[5]. k_{pe} strongly depends of the position along the x-axis and vanishes if the entrance length is reached.

Substituting Eq. (1) by Eq. (4), Eq. (12) and Eq. (13) the final differential equation for the change of pressure along the channel axis

$$2\sigma \frac{dH}{dx} + \frac{\rho Q^2}{A^3}\frac{dA}{dx} - \frac{\rho Q^2 (k_{pf} + k_{pe})}{2D_h \,\mathrm{Re}_{D_h} A^2} = 0 \quad (14)$$

is obtained. To get the dimensionless form the lengths are scaled by the hydraulic diameter D_h and the channel width b. The liquid velocity is scaled by the characteristic velocity $v_0 = 2\sqrt{\sigma/\rho D_h}$, which is known from the capillary imbibition of liquid in a channel of two parallel plates. As shown by Dreyer[6] this velocity cannot be exceeded. With $x^* = 4x/D_h$, $l^* = 4l/D_h$, $4H^* = D_h H$, $k^* = 4k/D_h$, $R = 4R/D_h$, $A^* = 2A/D_h b$, $v^* = v/v_0$, $Q^* = Q/\sqrt{\sigma D_h b^2/\rho}$ the dimensionless form of Eq. (14) reads

$$2\frac{dH^*}{dx^*} + \frac{Q^{*2}}{A^{*3}}\frac{dA^*}{dx^*} - \frac{\mathrm{Oh}}{8} Q^* (k_{pf} + k_{pe}) = 0. \quad (15)$$

The dimensionless parameters are the OHNESORGE number $\mathrm{Oh} = \mu/\sqrt{D_h \rho \sigma}$ and the aspect ratio $\Lambda = b/a$ occurring in the non-dimensional relation of the cross section $A^* = g_2^*(R^*)$. Eq. (15) has to be solved numerically taking into account the boundary conditions which are

$$k^*\big|_{x^*=0} = k^*\big|_{l^*=0} = \Lambda, \quad (16)$$

$$2H^*\big|_{x^*=0} = 2H_o^*, \quad (17)$$

the position of the surface at the inlet and outlet of the channel Eq. (16) and the surface curvature at the channel inlet Eq. (17). The numerical solution yields the position of the liquid surface

$$k^* = f(\Lambda, \mathrm{Oh}, l^*, Q^*). \quad (18)$$

Eq. (18) shows that the surface position depends on the adjusted volume flux Q^*. For each set of Λ, Oh, and l^* several model computations with different Q^* are performed. We assume that the maximal volume flux is reached when the numerical integration diverges. As the maximal theoretical volume flux Q_{crit}^* we define the maximal volume flux Q^* leading to the convergence of the numerical algorithm. Obviously the following relations

$$Q_{crit}^* = f_1(\Lambda, \mathrm{Oh}, l^*) \quad (19)$$

$$v_{crit}^* = f_2(\Lambda, \mathrm{Oh}, l^*) \quad (20)$$

are valid. $v_{crit}^{\cdot}$ is the corresponding critical mean velocity $v_{crit}^{\cdot} = Q_{crit}^{\cdot}/A_{min}^{\cdot}$ which occurs at the smallest cross section $A_{min}^{\cdot}$ of the liquid flow.

From another point of view we expect that the limitation of the flow rate occurs due to choking. The theory of choked flow predicts a limiting velocity corresponding to a characteristic signal velocity of the flow. In compressible gas duct flows the limiting speed is defined by the speed of sound. The characteristic number is the MACH number (Ma), and the maximal flow passes through the duct when Ma = 1 is reached locally.[7] In open channel flow dominated by normal gravity the speed of shallow water waves correspond to the limiting velocity, and choking occurs when the FROUDE number (Fr) becomes unity. Both wave speeds are derived from the general form

$$c = \sqrt{Adp/d(\rho A)}. \tag{21}$$

Eq. (21) is the wave speed of longitudinal waves in compressible flow with variable cross section.[8] A close analogy exists between both flow types which might be expandable to open capillary flows investigated in the present work. To show that the flow rate limitation is caused by choking, we scale the mean liquid velocity by the characteristic wave speed of the open capillary channel. Applying Eq. (3) and Eq. (10) to Eq. (21) the wave speed of the capillary open channel is

$$v_c = \sqrt{\frac{\sigma}{\rho}\frac{A}{R^2}\frac{dR}{dA}}. \tag{22}$$

Here we neglected the surface curvature in flow direction assuming

$$k_{xx} \simeq 0,\ k_x \ll 1, \tag{23}$$

which is valid in pieces along the channel in sufficient distance to the inlet and outlet. With the relations Eq. (6) and Eq. (7) the wave speed can be calculated from the experimental determined surface contour $k(x)$. Scaling the mean liquid velocity $v = Q/A$ by Eq. (22) the dimensionless parameter

$$\mathrm{We} = Q/Av_c = v/v_c \tag{24}$$

is defined, which is a WEBER number. Due to the above mentioned analogy we expect that the WEBER number tends towards unity when the flow rate becomes maximal.

EXPERIMENTS

The objective of the experimental investigations was to determine the maximum liquid volume flux

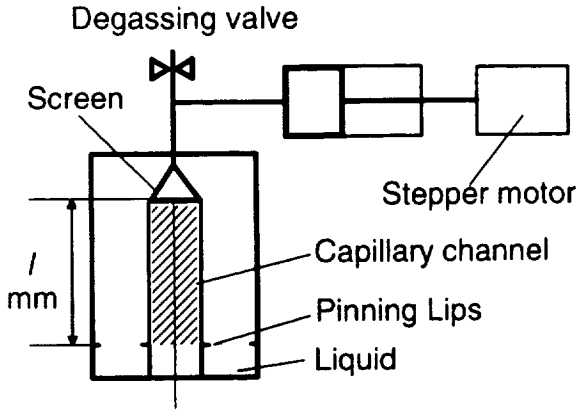

Figure 3: Schematic drawing of the experiment setup for the drop tower. During the microgravity period the capillary channel fills itself and pumping starts when the meniscus reaches the screen.

which can be sucked through open capillary channels, consisting of two parallel plates. To eliminate the gravity effects and to establish a liquid path between the parallel plates by means of the surface tension only, the experiments were performed under microgravity conditions in a drop tower and in a sounding rocket. In addition several preliminary investigations and component tests for the sounding rocket experiment were carried out in two flight campaigns in a parabolic aircraft.

The first experiments were performed in a drop tower and based on the experiments of capillary liquid rise between two parallel plates, Dreyer et. al.[6,9]. In essence the experiment setup consisted of a circular container, which was filled with a test liquid up to a certain height as shown in Fig. (3). Inside the container a channel of two parallel plates was fixed on the bottom, so that under normal gravity conditions the longitudinal channel axis was perpendicular to the liquid surface. On the top of the channel a withdrawal device consisting of a piston with stepper motor was mounted. The experiment setup was integrated in a drop capsule at the Bremen Drop Tower providing an experiment time of 4.74 s at a residual acceleration of $< 10^{-5}g$. Before the drop the withdrawal device was filled with the test liquid up to the screen, but the gap between the plates upside the liquid surface was empty. With the release of the capsule the liquid started to rise between the plates. This liquid movement is caused by the capillary pressure gradient between the liquid surface inside the container and the liquid surface inside the gap of

the plates. When the liquid meniscus contacted the withdrawal device the stepper motor started and a defined constant volume flux was withdrawn from the channel by means of the piston. Depending on the adjusted volume flux two typical observations were made. Below the critical value of the volume flux Q_{crit} ($Q < Q_{crit}$) the flow between the plates is stationary. Above the critical value ($Q > Q_{crit}$) the surface collapses and gas ingestion occurs. Based on this observation* we define the maximum volume flux as

$$Q_{crit} = 0.5(Q_{bc} + Q_{ac}), \qquad (25)$$

where Q_{bc} is the maximum experimental volume flux leading to a stable flow and Q_{ac} the minimum experimental volume flux leading to a the surface collapse.

Several experiments with various liquids and different channel properties were performed. Since the result of this work shall be useful for surface tension tanks, the experimental parameter were chosen with respect to propellant data (N_2O_4 and MMH) and tank geometries. Satellite tanks usually operate in the temperature range $T = 0 \ldots 40$ °C and typical geometries are: gap distances $a \approx 1 \ldots 10$ mm, plate breadths $b \approx 10 \ldots 30$ mm. This leads to the parameter field given by the combination $0.427 \cdot 10^{-3} \leq \mathrm{Oh} \leq 5.881 \cdot 10^{-3}$ and $3 \leq \Lambda \leq 10$. The experiment parameters are given in Table 1 and

Table 1: Experiment parameters for Bremen drop tower experiments with experiment time of 4.74 s.

#	Fluid	a/cm	b/cm	l/cm
1	SF 1.0	0.5	3	9.5 ± 0.05
29	FC-77	0.2	2	7.5 ± 0.1
32	SF 0.65	0.3	1	9.45 ± 0.05
33	SF 0.65	0.3	1.5	9.6 ± 0.05
34	SF 0.65	0.3	3	9.45 ± 0.05
35	SF 0.65	0.5	2.5	9.5 ± 0.05
35a	SF 0.65	0.5	2.5	4.8 ± 0.05
36	FC-77	0.2	1	7.5 ± 0.1

Table 2. All fluids show perfectly wetting behavior at the capillary walls. Laminar flow conditions were expected for all experiments since the REYNOLDS number was sufficiently small. The combination of flow length l and maximum volume flux Q must be chosen with respect to the experiment constraints: overall experiment time (4.74 s), capillary rise time to fill the channel compared to pumping time, optical resolution of the surface contour (depends on the gap distance a). Due to the short experimental time the OHNESORGE number was restricted to $\mathrm{Oh} \geq 1.52 \cdot 10^{-3}$ (#35).

*A detailed explanation is given below, when the sounding rocket experiment is discussed.

Table 2: Dimensionless parameters for the drop tower experiments.

#	Λ	Oh	l^*	Re_{D_h}
1	5.99	0.00238	0.045	534
29	3.33	0.0047	0.177	156
32	3.33	0.00197	0.062	578
33	5	0.00197	0.063	600
34	10	0.00197	0.062	625
35	5	0.00152	0.029	909
35a	5	0.00152	0.015	977
36	5	0.00472	0.177	151

The maximum volume flux was determined for each parameter set. Theoretical model computations were performed under the assumption of Eq. (23) and a different factor k_{pe}. The calculations show a good agreement with the experiments with respect to the maximum volume flux and the predicted surface contour. However, due to the transition from the self-driven capillary flow to the forced flow inertia effects occurred which made an exact approach of the critical value impossible. Furthermore, the established volume flux had to be kept constant since the short experimental time did not allow an increase of the volume flux. More details regarding the experiment setup and the results are discussed by Dreyer et. al.[10].

To operate under longer μg-time an experiment module was flown on the sounding rocket TEXUS-37 providing a microgravity environment of 10^{-4} g in all axis for approximately 6 minutes. The module was equipped with a pump system that allowed the increase of the volume flux in small steps (quasistatic approach) to minimize the transient inertia effects.

A schematic drawing of the experiment cell is shown in Fig. 4. It consists of the liquid reservoir with compensation tube and the observation chamber with the channel ($a = 5$ mm, $b = 25$ mm, $l = 47$ mm). The flow is established by two gear pumps. One pump supplies the reservoir through a circular gap on the bottom of the reservoir (volume flux Q_1). Via the nozzle, the liquid is conducted into the capillary channel. At the channel outlet the volume flux Q_2 is withdrawn by the suction pump. The difference of both volume fluxes caused by fluctuations of the rotation speed and varying liquid slip inside the pump is compensated by the compensation tube.

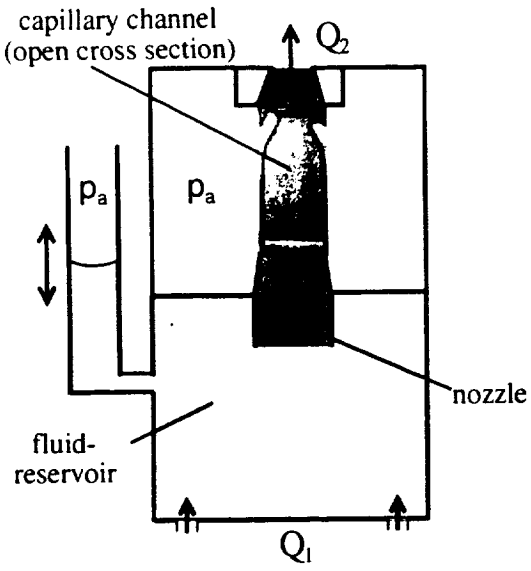

Figure 4: Schematic drawing of the TEXUS experiment module.

Furthermore the liquid meniscus in the tube sets the pressure in the reservoir and defines the boundary condition at the channel inlet Eq. (17) needed to solve Eq. (15). To prevent the meniscus disappearing into the reservoir the supply pump was adjusted to pump a 3% higher volume flux than the suction pump. With this adjustment, the liquid rose continuously in the compensation tube. Each pump is connected to a separate reservoir for the test liquid supply and the storage of withdrawn liquid.

The experiment was observed by three CCD cameras. The video signals were down linked to the ground and recorded on a VCR (S-VHS quality). Additionally the camera view of the compensation tube was recorded on board by a DV camcorder. Two cameras were used for the observation of the channel (made from quartz glass) yielding a resolution of approximately 0.05 mm/pixel. Both sections of image had an overlap of 10 mm. On the front plate markings were etched for the calibration of pictures and the check of the optical resolution.

The experiment was controlled manually during the flight of the sounding rocket. All hand-controlled procedures necessary for the TEXUS experiment control had been practiced during two parabolic flight campaigns. In the initial configuration before the lift off the compensation tube and the nozzle were each closed with a gate valve, both pumps were off. Once under microgravity conditions, the capillary channel was filled. To avoid wetting outside the channel caused by an uncontrollable liquid jet, the channel was not filled directly by the pressure pump but by the self-driven capillary rise, which was well-known from the drop tower experiments. For that reason, the compensation tube was filled first. After opening the gate valve at the nozzle the liquid rise occurred and the channel filled itself. When the liquid reached the channel outlet it was withdrawn by the second pump. By starting the first pump a continuous flow through the open channel was established.

The filling procedure took approximately 30 s. In the remaining experimental time the volume flux was increased up to the critical value. In contrast to the drop tower experiment the change of volume flux by each step is small, and the inertia effects are sufficiently smaller since the channel is supplied by the two synchronized pumps. The experiment provided the options to change the volume flux in 0.1 ml/s or 0.05 ml/s steps. At first the bigger step size for a rough approach was chosen to save experiment time. After the gas ingestion was observed the volume flux was decreased and a second approach was performed at small steps of volume flux. The typical observations, which are the same for the drop tower experiments, are shown in Fig. 5 and Fig. 6. The camera view is perpendicular to the top plate. Since the plates are transparent the free surface appears as a dark contour, which corresponds to the distance h defined in Fig. 2. Below the critical value of volume flux Q_{crit} ($Q < Q_{\text{crit}}$) the flow between the plates is stationary. The free surface is stable and the corresponding innermost line of the surface is constant in time, $k = k(x)$. For $Q > Q_{\text{crit}}$ the surface collapses and gas ingestion occurs. The free surface becomes time-dependent, $k = k(x,t)$. The withdrawn total flux now is a superposition of the maximum liquid volume flux and an additional volume flux of gas.

Prior to the experiment, we performed three-dimensional model computations using the finite element code FIDAP[11]. The computations were necessary to optimize the flow conditions inside the liquid reservoir and the nozzle as well as to calculate the pressure loss caused by both components. With the knowledge of the pressure loss the pressure at the channel inlet and the related boundary condition from Eq. (17) (necessary to solve Eq. (15)) is defined. Both liquid surfaces in the compensation tube and in the channel are exposed to ambient pressure. For this reason the inlet pressure is determined by the ambient pressure minus the static capillary pressure of the liquid surface in the compensation tube and the dynamic flow losses, which

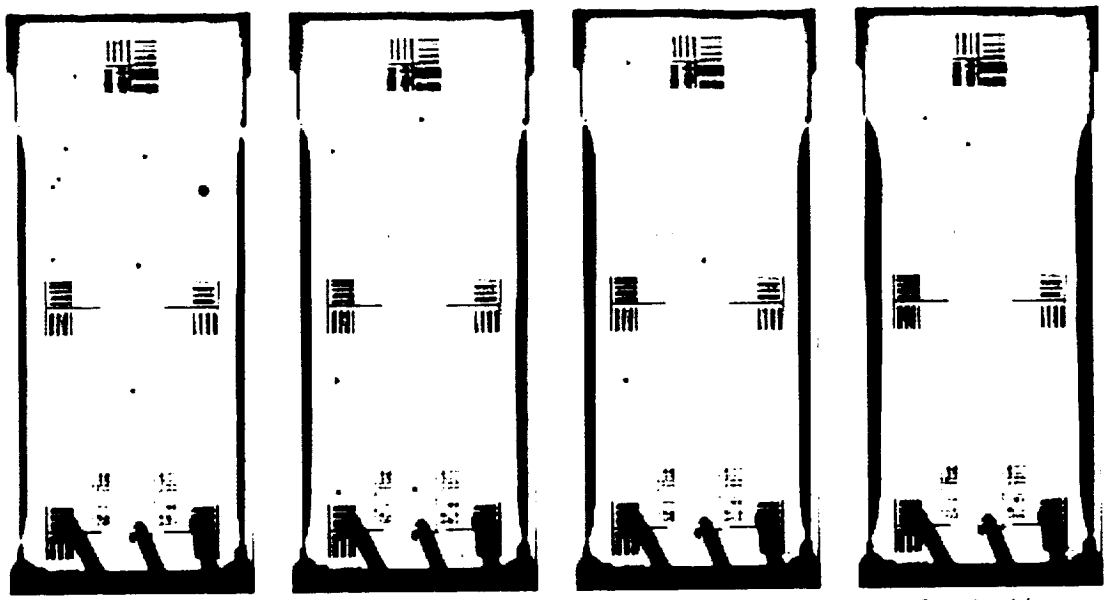

Figure 5: Stable volume flux during the TEXUS experiment, $Q < Q_{crit}$. The camera view is perpendicular to the front plate as shown in Fig. 2. Since the plates are transparent the free surface appears as a dark contour. The flow direction is from the bottom to the top. With increasing volume flux the surface curvature increases along the channel axis and the flow path becomes smaller.

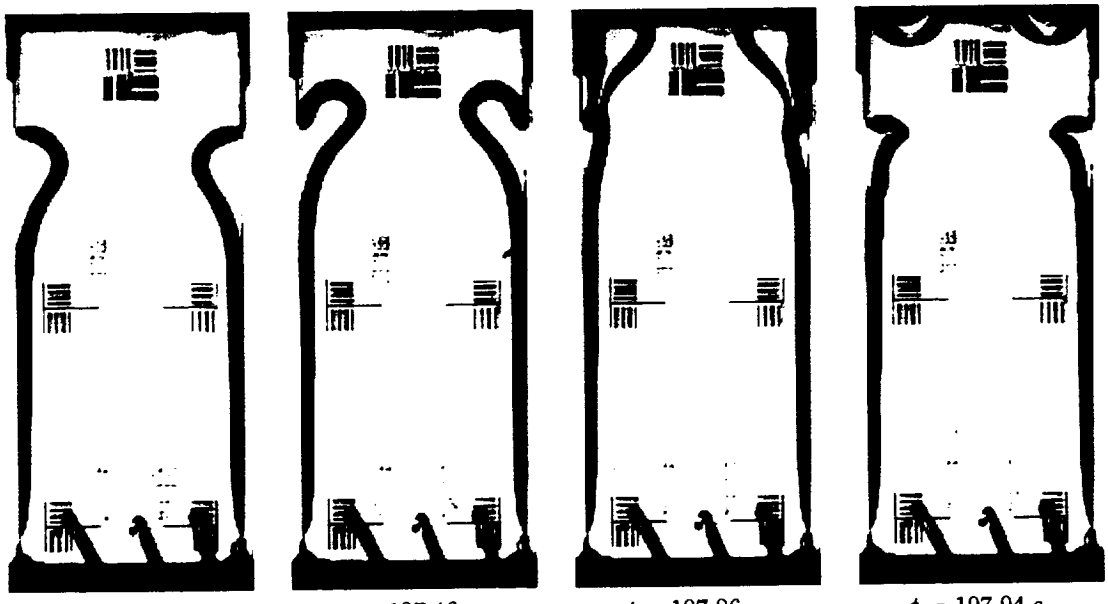

Figure 6: Unstable liquid flow in a capillary channel between two parallel plates during the TEXUS experiment. The adjusted volume flux lies above the critical value $Q > Q_{crit}$. The differential pressure between the liquid and ambient cannot be compensated by the capillary pressure of the liquid surface. The surface collapses and gas ingestion occurs.

was fitted to

$$2H_0^* = k_1 + k_2 Q^* + k_3 Q^{*2} \qquad (26)$$

in terms of the surface curvature. The constant $k_1 = 0.222$ considers the capillary pressure of the compensation tube (inner diameter 45 mm). Since the test liquid is perfectly wetting, the shape of the surface inside the tube is a section of a sphere culotte. The factors $k_2 = 0.128$ and $k_3 = 0.725$ represents the dynamic losses due to friction and convective acceleration.

RESULTS

During the 6 minute flight the experiment module worked well. The filling procedure and all experiment procedures were performed on schedule. No leakage of liquid into the observation chamber occurred, even though the pumps were stopped abruptly. After the flow through the channel was established, the volume flux was increased up to the critical value twice. With the first approach at the bigger step size the surface collapsed at $Q = 9.1$ ml/s. At the same value of Q the second approach with smaller steps yielded a stable flow, which could not be increased further since the experimental time expired, thus the critical volume flux by the definition of Eq. (25) was not obtained. However, this effect shows how sensitive the flow responds to inertia effects at this stage.

Several stable flow configurations at different volume flux Q below the critical value were observed as shown in Fig. 5. As expected the distance h increased with increasing volume flux and the liquid flow path became smaller. The highest volume flux leading to a stationary flow could be realized at $Q_{bc} = 9.1$ ml/s. The recorded video pictures are processed by digital imaging tools so that the innermost line $k(x)$ is available for each stable volume flux ($Q < Q_{crit}$). For each Q during the experiment Eq. (15) with the boundary conditions from Eq. (26) was solved. The comparison with the surface contour data is shown as an example in Fig. 3 for a low and a high volume flux at $Q = 6$ ml/s and $Q = 9$ ml/s, respectively. The evaluated surface positions at different times are represented by the black terraced lines. Slight surface vibration caused by the gear pumps are observed. The solid line is the theoretical prediction of k. The figures show that computations predict the volume flux and corresponding the surface position in good agreement with the experimental data.

To show the influence of the WEBER number from Eq. (24), the waves speed v_c Eq. (22) and the

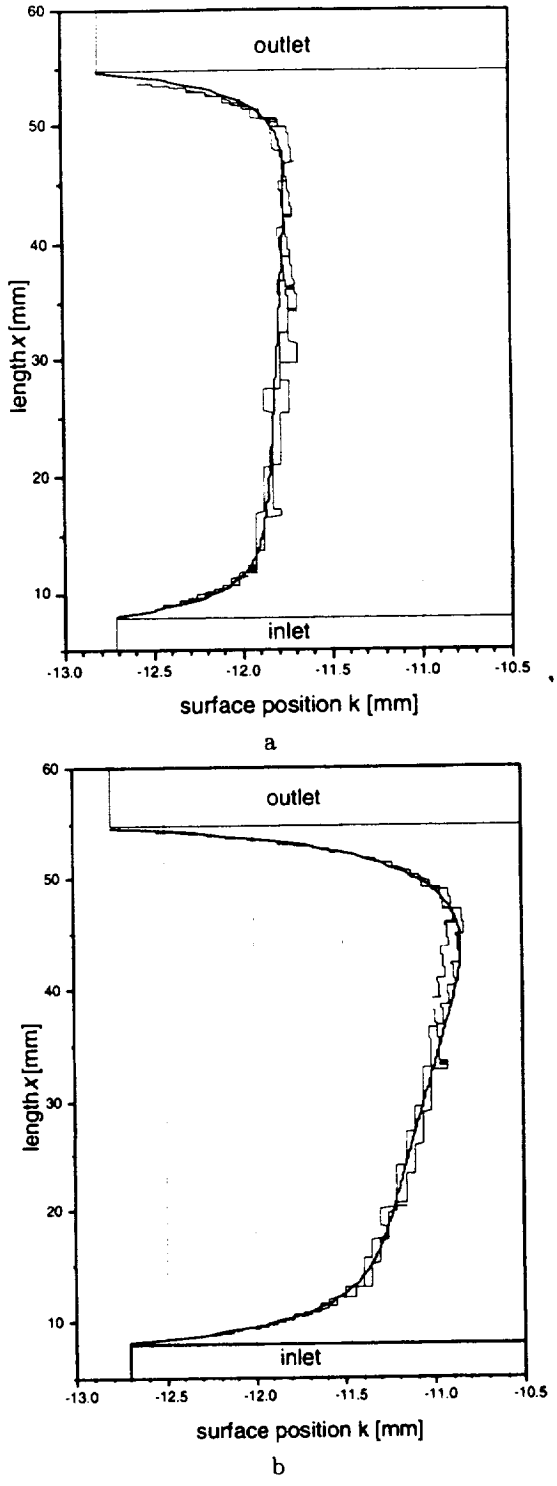

Table 3: Evaluated surface contour from the TEXUS experiment (thin lines). Slight surface vibrations caused by the gear pumps are observed. The thick solid line shows the theoretical prediction (a: $Q = 6$ ml/s, b: $Q = 9$ ml/s).

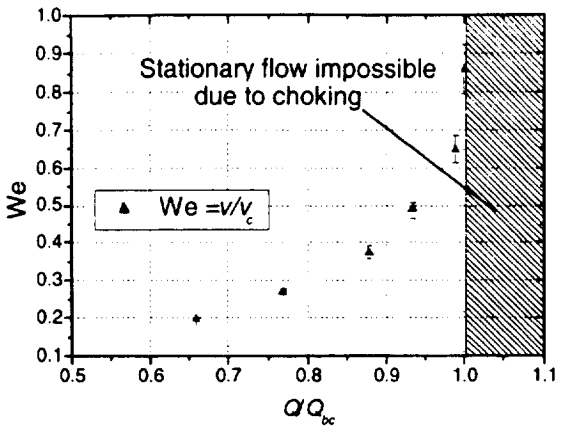

Figure 7: WEBER number as function of the adjusted volume flux. At We = 1 the flow is choked and a further increase of volume flux is impossible.

mean liquid velocity $v = Q/A$ are calculated from the experimental data of the surface position $k(x)$. Using the relations Eq. (6) and Eq. (7) both velocities are determined. Since the effect of choking is expected to appear at the location of minimum liquid pressure, the WEBER number was calculated at the smallest cross section $A_{\min} = A(k_{\min})$. The analysis shows that with increasing volume flux the liquid velocity increases, but the characteristic wave speed decreases. Therefore, the WEBER number tends towards unity as the theory of choking predicts (Fig. 7). At the maximum stable volume flux ($Q_{\mathrm{bc}} = 9.1$ ml/s) the corresponding WEBER number yields We = 0.86. Fig. 7 indicates that the flow runs very close to the critical condition, since a small change of volume flux causes a large variation of the WEBER number at this stage.

OUTLOOK

As we have demonstrated in the drop tower and sounding rocket experiments, much longer microgravity durations are necessary to fully span the parameters discussed in this paper. Furthermore, very small incremental increases in flow rates are required to minimize the transient inertial effects. In order to meet these requirements, this experiment has been tentatively selected as a definition-phase flight experiment for the ISS. The experimental hardware will be developed and built at the Center of Applied Space Technology and Microgravity (ZARM) and integrated into the Fluids Integrated Rack (FIR). The FIR is a component of the Fluids and Combustion Facility (FCF) and will be located in the US laboratory module, Destiny.

We will take advantage of both the 30 fps high resolution digital black and white camera package and the Ultra High Frame Rate (UHFR) camera. We will also make use of the Command and Data Management Subsystem (CDMS) to control and measure liquid and gas flow rates, temperatures and pressures. Integration and testing into the FIR is tentatively scheduled for 2006.

CONCLUSION

The aim of the experiments was to investigate the flow rate limitation in open capillary channels. In spite of the applications of capillary channel (vanes) in surface tension tank technology the basic physics leading to the flow rate limitation is not well-known. Experimental and theoretical data on this research field are rare. To eliminate the hydrostatic pressure the experiments were performed under the microgravity environment of the Bremen Drop Tower and on board the sounding rocket TEXUS-37. The investigated dimensionless characteristic numbers cover a wide range of usual vanes. For the theoretical approach a one-dimensional momentum balance was set up, which yields the maximal volume flux and the position of the free surface $k(x)$. Both the calculated volume flux and the surface position are in good agreement with the experimental data. Furthermore the experiment on board TEXUS-37 showed that the limitation of flow rate occurs due to choking indicated by the WEBER number. Since the characteristic wave speed v_c was derived from the general waves speed Eq. (21) the capillary open channel flow is analogous to MACH number and FROUDE number problems. For the entire understanding of the mechanism of flow rate limitation in open capillary channels the parameter field to be investigated must be expanded. To keep the influence of inertia effects smaller the increments of volume flux have to be reduced leading to longer experimental times. In order to meet these requirements, this experiment has been tentatively selected as a definition-phase flight experiment for the ISS.

ACKNOWLEDGEMENT

The funding of the drop tower flights and the sounding rocket flight by the European Space Agency (ESA) and support of the work by the German Aerospace Center (DLR) is gratefully acknowledged. Thanks are due to Mr. Prengel for the experimental setup and the performance of the drop tower flights.

NOMENCLATURE

a	distance between the parallel plates
b	breadth of parallel plates
g	gravitational acceleration
c	longitudinal wave speed in fluids with variable cross section
h	height of circle segment
k	position of the innermost surface line
$k_{\min}$	minimum position of the innermost surface line
k_{pf}	factor of the laminar pressure loss, $k_{\mathrm{pf}} = 96$
k_{pe}	factor of the entrance pressure loss
l	length of capillary channel
p	pressure
p_{a}	ambient pressure
v	average velocity in direction of the flow path
v_0	characteristic velocity, $v_0 = \sqrt{2\sigma/\rho a}$
v_c	longitudinal wave speed in open capillary flow
v_{crit}	critical flow velocity
w_{f}	energy loss of the flow
x	channel co-ordinate, flow path co ordinate
y	channel co-ordinate
z	surface position
A	cross section area of the flow path
$A_{\min}$	minimum cross section area of the flow path
D_h	hydraulic diameter, $D_h = 2a$
Fr	FROUDE number
H	mean surface curvature
H_0	mean surface curvature at the chanel inlet
Q	volume flux
Q_{ac}	minimum experimental volume flux leading to the surface callapse
Q_{bc}	maximum experimental volume flux at stable flow condition
Q_{crit}	critical volume flux
Oh	OHNESORGE number, Oh= $\mu/\sqrt{D_h\rho\sigma}$
R	radius of curvature
$R_{1,2}$	main radii of curvature
Re_{D_h}	Reynolds number based on the hydraulic diameter, $\mathrm{Re}_{D_h} = D_h v/\nu$
Ma	MACH number
We	WEBER number, We= v/v_c
ρ	density
μ	dynamic viscosity
ν	kinematic viscosity
σ	surface tension
Λ	gap ratio, $\Lambda = b/a$
$*$	dimensionless quantiy

REFERENCES

1. Jaekle, D.E., Propellant Management Device Conceptual Design and Analysis: Vanes, AIAA-91-2172, 27th Joint Propulsion Conference, June 24-26, Sacramento, CA, USA (1991).
2. Der, J., A linearized Theory for Unsteady Surface Tension Driven Flow along Supercritical Vane-formed Fillets, AIAA-91-2175, 27th Joint Propulsion Conference, June 24-26, Sacramento, CA, USA (1991).
3. Bronstein, I.N., Semendjajew, K.A., *Taschenbuch der Mathematik*, Teubner, Leipzig (1985).
4. White, F.M., *Fluid Mechanics*, McGraw Hill, New York 1986, p. 323.
5. E. M. Sparrow, S. H. Lin, Flow Development in the Hydrodynamic Entrance region of Tubes and Ducts, Phys. Fluids Vol. 7, Nr. 3, 1964.
6. Dreyer, M., Delgado, A., Rath, H.J., Capillary Rise of Liquid between Parallel Plates under Microgravity. J. Colloid Interf. Sci. **163**, 158-168 (1994).
7. Shapiro, A.H., *The Dynamics and Thermodynamics of Compressible Fluid Flow*, Vol. 1. The Ronald Press Company, New York (1953).
8. Lighthill, J., *Waves in Fluids*, Cambridge University Press, Cambridge (1978).
9. Dreyer, M., *Kapillarer Flüssigkeitsanstieg zwischen parallelen Platten unter kompensierter Gravitation*, Dissertation Universität Bremen, Fortschritt-Berichte VDI, Reihe 7 Nr. 241, Düsseldorf: VDI-Verlag (1994)
10. Dreyer, M.E., Rosendahl, U., Rath, H.J., Experimental Investigation on Flow Rate Limitations in Open Capillary Vanes, AIAA 98-3165 (1998).
11. FIDAP Version 7.5, User´s Manual, Fluid Dynamics International Inc. 1995.